

**Texas A&M University
Mechanical Engineering Department
Turbomachinery Laboratory
Tribology Group**

**ISSUES AND CONSIDERATIONS FOR THE ACCURATE
MODELING OF LONG, GROOVED ANNULAR SEALS
FOR PUMPS**

A Report to the Turbomachinery Research Consortium

TRC-SEAL-02-15

By

Luis San Andrés
Mast-Childs Chair Professor
Principal Investigator

Tingcheng Wu
Research Assistant

May 2015

Executive Summary

Issues and Considerations for the Accurate Modeling of Long, Grooved Annular Seals for Pumps

This report reviews the development of models, bulk-flow and CFD based, applied to the prediction of flow and force coefficients in grooved annular seals for pumps. XLTRC² XLCGrv[©] bulk flow model uses friction factor coefficients, $f=n Re^m$, with Re as a flow Reynolds number, and n and m derived from test data. For short length grooved seals ($L/D < 0.45$), XLCGrv[©] predictions agree with experimental force coefficients obtained at TAMU over 20 years ago. For long seals ($L/D > 1$) with shallow grooves, XLCGrv[©] predictions are regarded (by industry) as inadequate to reproduce field behavior in a boiler feed pump.

CFD solutions to the complex flow in grooved seals are (becoming) common engineering practice as commercial software is readily accessible and computers' processing speed continuously increases. However, prediction of seal force coefficients using commercial CFD software still demands of a large intellectual effort and computing time.

A CFD/Bulk Flow hybrid analysis method is outlined to predict the dynamic force coefficients of annular seals handling a liquid and with grooved configurations of shallow depth, as they seem to be preferred by pump manufacturers. The method has been show to deliver better (more accurate) force coefficients than bulk-flow predictions for a long seal (balance piston), as derived from indirect comparisons to rotordynamic test data available for a commercial pump.

Table of Contents

EXECUTIVE SUMMARY	Error! Bookmark not defined.
Table of Contents	3
List of Figures	4
List of Tables	5
Nomenclature	6
1. Introduction.....	7
2. Literature Review.....	9
2.1 Introduction of Bulk-Flow Model.....	9
2.2 Analysis for Grooved Seal with Bulk-Flow Model	11
3. Analysis for Grooved Seal with Existing XLCGrv [®] Program.....	13
3.1 Predictions for Short Length Grooved Annular Seals.....	14
3.2 Predictions for Long Grooved Annular Seals ($L/D > 1$)	16
4. Analysis for Grooved Long Seal with CFD software.....	16
5. A CFD/Bulk-Flow Hybrid Method.....	20
6. Closure	21
References.....	22

List of Figures

Figure 1. Geometry of a circumferentially grooved annular liquid seal.....	7
Figure 2. Pipe flow: Friction factor vs Reynolds number [9].....	10
Figure 3. Florjancic's three-control-volume model for flow in a grooved liquid seal [11].....	12
Figure 4. Experimental and predicted radial force (f_r) versus shaft speed for seals 1 and 7 in Kilgore [17].....	15
Figure 5. Experimental and predicted tangential force (f_θ) versus shaft speed for seals 1 and 7 in Kilgore [17].....	15
Figure 6. Cross section of seal with a whirling rotor.....	18

List of Tables

Table 1 Dimensions of Halon seals tested by Kilgore [19]	14
Table 2 Seal geometry, boundary conditions and flow parameters reproduced from Untaroiu <i>et al.</i> study [24]	18
Table 3 Dynamic force coefficients from CFD and Bulk-Flow methods. Data reproduced from Untaroiu <i>et al.</i> study [24 [24]	18
Table 4 Pump operating conditions for Untaroiu <i>et al.</i> rotordynamic study [24]	20

Nomenclature

c	Seal radial clearance [m]
c_g	Groove depth [m]
L_g	Groove length [m]
L_l	Land length [m]
D	Seal diameter [m]
R	Rotor radius [m]
L	Seal length [m]
ω	Rotor speed [RPM]
Ω	Whirl speed [RPM]
F	Force [N]
U	Circumferential velocity [m/s]
V	Radial velocity [m/s]
W	Axial velocity [m/s]
Re	Reynolds number
f_r, f_θ	Radial, tangential force [N]
K	Stiffness coefficient [N/m]
C	Damping coefficient [N*s/m]
M	Added mass coefficient [kg]
P_s	Supply pressure [Pa]
P_a	Ambient pressure [Pa]
\dot{Q}	Leakage flow [m ³ /s]
μ	Dynamic viscosity [Pa*s]
ν	Kinematic viscosity [m ² /s]
τ	Shear stress [N/m ²]
ρ	Mass density [kg/m ³]

1. Introduction

Multistage centrifugal pumps and compressors are among the most widely used products of rotating machinery in industry. A typical application demands the arrangement of several impellers or wheels mounted on a shaft that spins within a stationary case. Annular seals are the most common sealing devices utilized in this type of machinery. Because of the interaction within the rotor and the stator through the fluid flow within the seals, the annular seals design affects both the energy conversion efficiency and the system rotor dynamic stability.

Figure 1 illustrates a typical circumferentially grooved annular liquid seal; deep grooves break the seal land and thus reduce the seal cross-coupled stiffnesses [1]. Nordmann (1986) [2] conducts both theoretical and experimental research on the rotordynamic coefficients of parallel groove seals. Compared with smooth annular seals, Nordmann shows a grooved seal has less leakage and less cross-coupled stiffness. Deep grooving patterns (groove depth to clearance ratio, $C_g/C_r \cong 1$ or greater) can reduce direct stiffness and damping substantially. Too shallow grooves or too deep grooves do not reduce direct stiffness and damping appreciably [2, 3].

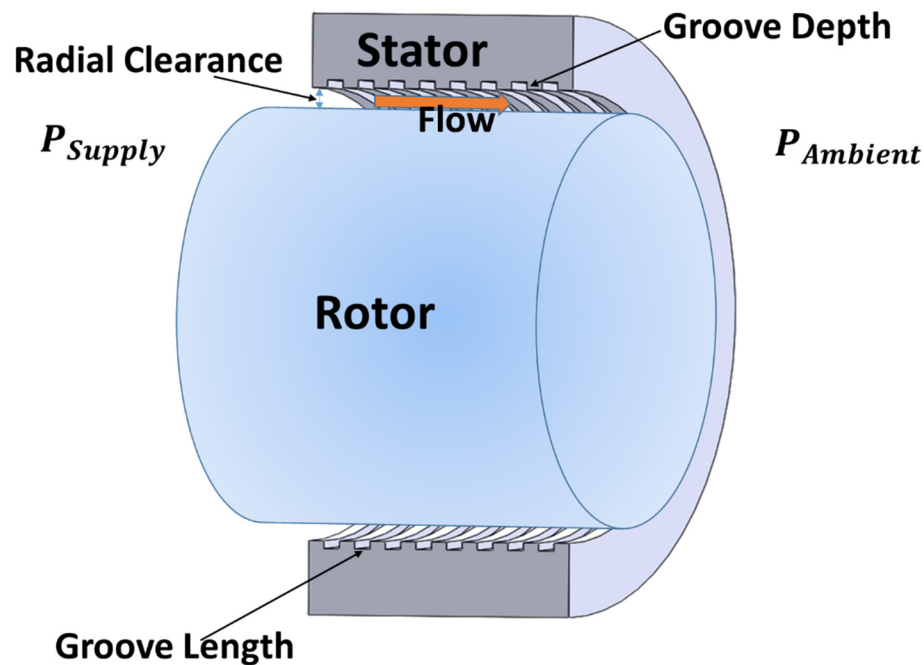


Figure 1. Geometry of a circumferentially grooved annular liquid seal.

In the past, researchers have employed both experimental and numerical methods to predict the performance of grooved annular seals. In past years, the bulk-flow model was widely used in

numerical studies. From a fundamental fluid mechanics perspective, the flow patterns in a circumferentially grooved annulus are considerably more complex than in a smooth land (not grooved) configuration. Thus, a bulk-flow model approach was unlikely to yield a realistic or accurate characterization of rotor vibration coefficients for circumferentially grooved seals [4]. Nordmann and Dietzer (1990) [5] use a finite difference solution of the Navier-Stokes equations with turbulent flow in mesh configurations reproducing a deeply grooved seal. Comparisons between their computational predictions and experimental results reveal good correlation. At the time of their work, computer costs were a significant factor in obtaining accurate Navier-Stokes solutions. With the fast development and ready availability of computational fluid dynamic (CFD) programs, as well as present workstations and top-end PCs, such computational costs are no longer a significant consideration.

This report reviews the development of models, bulk-flow and CFD based, applied to the prediction of flow and force coefficients in grooved seals. Force coefficient predictions for long grooved seals by an existing bulk-flow model program, XLCGrv© in the XLTRC² software suite, show poor correlation with pump rotordynamic data [6]. CFD method predictions of rotordynamic coefficients show good accuracy [7], but the computational cost of a CFD solution is higher compared to that of XLCGrv®. A CFD/bulk-flow hybrid analysis method is a happy compromise to predict the rotordynamic coefficients with a good accuracy and computational efficiency.

2. Literature Review

2.1 Introduction to the Bulk-Flow Model

In 1973, Hirs [8] proposed the bulk-flow theory for modeling flow turbulence in thin film flows. The bulk-flow model relies entirely on empirical information obtained from experiments. Hirs's theory sought to relate the wall shear stress differences to the mean flow velocity components across the film thickness. As Hirs states, "*the bulk-flow theory is based on the empirical finding that the relationship between wall shear stress and mean flow velocity relative to the wall at which the shear stress is exerted can be expressed by a common, simple formula for pressure flow, shear flow, or a combination of these two basic types of flow.*"

At the time, published research reported drag losses in pipe flow, shear drag between rotating cylinders, and pressure (extrusion) flow within stationary plates. The empirical research revealed that, for sufficiently large Reynolds numbers (Re), the wall shear stress can be expressed as [8]

$$\frac{\tau}{\frac{1}{2}\rho U_M^2} = f = n_0 \left(\frac{\rho U_M h}{\mu} \right)^{m_0} \text{sgn}(U_M) = n_0 Re_M^{m_0} \text{sgn}(Re_M) \quad (1)$$

where U_M is the mean velocity of flow relative to the surface at which the shear stress is exerted, τ is the shear force, f is the friction factor. Above $Re_M = (\rho U_M h / \mu)$ is the Reynolds number for the mean flow relative to the wall with ρ as the density of fluid, μ as the absolute viscosity; and h is a characteristic film length. The coefficients (n_0 , m_0) are empirical values derived from curve fits to the experimental data.

The magnitude of the coefficients n_0 and m_0 typically depends on (1) roughness or texture of the lubricated surfaces; (2) curvature of the surfaces; (3) influence of inertia effects other than those inherent in the flow turbulence; (4) the type of flow: ①pressure flow, ②drag flow, ③ or the nature of the combination of both flow types [8, 9]. Hirs provides the following friction factor for smooth surfaces

$$\text{For pure pressure flow } (\tau_0), \quad m_0 = -0.25, n_0 = 0.066 \quad (2)$$

$$\text{For pure shear flow } (\tau_1), \quad m_0 = -0.25, n_0 = 0.055 \quad (3)$$

The general form of the friction factor could be written as $f = nRe^m$. The bulk-flow model can also be extended to consider textured bearing surfaces by an appropriate choice of the coefficients n and m . However, this procedure is quite cumbersome and rarely provides any

physical insight. The literature in turbulent flow seals and bearings with textured surfaces revises Hirs's approach and employs empirically based friction factors that account for the textured surface effects [3].

One simple form to extract friction factor directly is from a curve fit of Moody's Diagram for pressure driven flow in pipes. This friction factor fitting to Moody's extensive empirical data is (Massey, 1983) [10]

$$f_i = \alpha \left[1 + \left\{ 10^4 \frac{r_i}{h} + \frac{5 * 10^5}{R_i} \right\}^{\frac{1}{e}} \right] \quad (4)$$

where $\alpha = 0.001375$, $e = 3.0$, $i = J$ (journal), or B (Bearing) surfaces, and r corresponds to the surface roughness. The equation above is strictly valid for surface roughness (r) to 10% of the local film thickness or clearance (h).

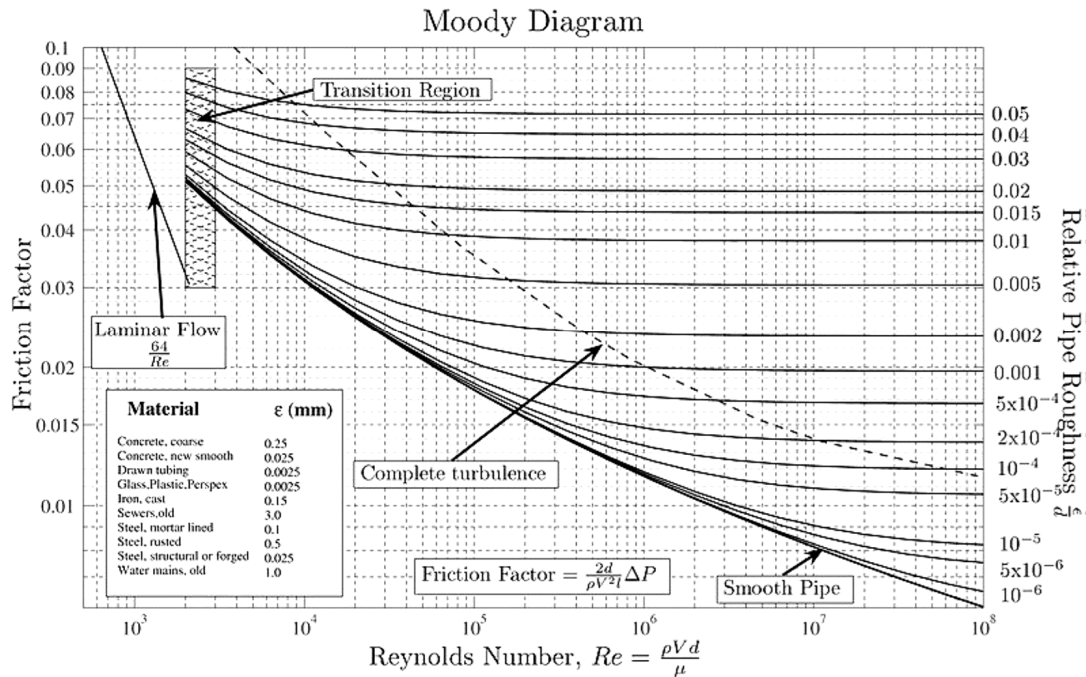


Figure 2. Pipe flow: friction factor vs Reynolds number [9].

Early analyses of turbulent flow in annular pressure seals present numerical predictions based on Moody's or Hirs's friction factors and compared them to measurements. In general, the

experimental-analytical correlation favors the model that employs Moody's friction factor (Nguyen, 1987) [11].

Hirs's turbulent bulk-flow, including fluid inertia effects, is used extensively to predict the flow characteristics and rotordynamic coefficients of annular pressure seals and externally pressurized bearings. In general, predictions correlate well with measurements for smooth surface seals and bearings.

Bulk-flow models use cross-film average for fluid pressure and flow velocities, while the wall shear stress is defined in terms of the wall friction factor. In general, Childs [3] notes a bulk-flow model will provide reasonable predictions of force coefficients for plain smooth land seals under lateral or tilting rotor displacements or their combination

Based on the method's simplicity, several authors have contributed to the bulk-flow approach; most recently, Arghir and Frene [12] extended the analysis of Florjancic [13] to analyze an eccentric circumferentially grooved liquid annular seal. Arghir and Frene [12] leakage predictions agree with the experiments of Marquette and Childs [3, 14, 15], within 2.5%, for a centered operation. On the other hand, dynamic coefficients are either over or under predicted, ranging from 20% to 120%.

Computational analyses based on the bulk-flow model for complex seal geometries such as labyrinth seals and honeycomb damper seals predict well the static characteristics (leakage mainly) but estimate rotordynamic force coefficients poorly. The friction factors in these seal configurations are more complicated functions of the Reynolds number and surface conditions than the simple formulas advanced by Hirs [8]. Note that the bulk-flow model does well in flows without strong recirculation zones or curved streamlines.

2.2 Analysis for Grooved Seal s with a Bulk-Flow Model

To estimate the dynamic force coefficients of seals with deliberately textured surfaces, most analyses use the bulk-flow approach, in which the wall shear stress is defined in terms of the friction factor. In the past, researchers developed various analyses for grooved annular seals based on Hirs's bulk flow model [8]. In 1986, Nordmann *et al.* [2] first develop a model that uses the minimum clearance for the axial-momentum equation and an average clearance for the circumferential-momentum equation. Nordmann determined the axial friction factor from the

leakage or axial pressure gradient data and treated the circumferential direction as a smooth surface [2, 3]. In 1990, Childs and Kilgore [14] report lengthy comparisons between the predictions of Nordmann's model [2] and their measurements for both the friction factor and rotordynamic coefficients.

In 1990, Florjancic [13] develops a bulk-flow model based on an extension of Scharrer's [16] solution for gas labyrinth seals to obtain predictions for grooved seals with a reasonable computational cost at the time. Florjancic implements a "three-control-volume" model, as illustrated in Figure 3. The author devises a bulk-flow mode in control volumes I and II and uses the Moody friction factor, and assumes a single vortex exists in control volume III. This vortex appears only for a deep groove geometry, with approximately equal width and depth, but several times the operating film clearance. In deeper grooves, multiple vortices will form, whereas in a long and shallow groove, the flow can reattach to the cavity prior to entering the next film land [3].

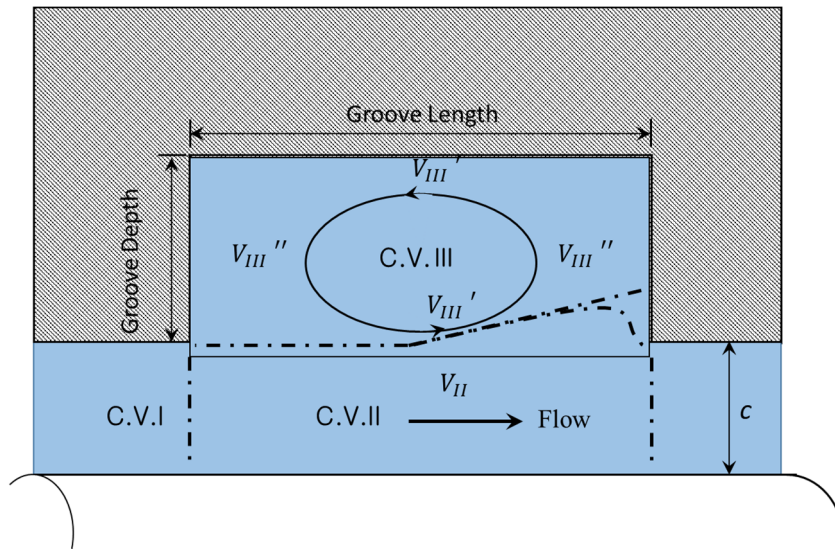


Figure 3. Florjancic's three-control-volume model for flow in a grooved liquid seal [13].

3. Analysis for Grooved Seals with XLCGrv[®] Program

In 1996, Marquette and Childs [17] developed the XLCGrv[®] program based on an extended three-control-volume model. The authors use the CVI (Control Volume I) to develop a standard bulk-flow model in the film land sections of the grooved seal. In CVI, Marquette and Childs express the shear stresses at the rotor and stator with Blasius formula

$$f = nR_e^m \quad (5)$$

where R_e is the Reynolds number relative to the wall and n and m are empirical constants. The constants for the rotor surface are (n_r, m_r) ; the constants for the stator surface are (n_s, m_s) . In CVI, the default values for the rotor and stator apply for smooth surfaces. In the groove section, Marquette and Childs model the through-flow section (CVII) with a bulk-flow model, and apply a vortex model in the groove (CVIII) with a vortex velocity equal to a fixed fraction of the axial velocity W_o in CVII [17, 18].

A friction factor model with the same coefficients (n, m) as in the land section defines the shear stresses acting on the rotor surface in CVII. On the other, shear stresses acting at the interface between CVII and CVIII are defined by a jet shear stress model of the form

$$\tau_{jz} = 1.88\rho\beta_z^2|V_{II} - V_{III}|(W_{II} - \overline{W_{III}}) \quad (6)$$

$$\tau_{j\theta} = 1.88\rho\beta_\theta^2|V_{II} - V_{III}|(U_{II} - U_{III}) \quad (7)$$

where the parameters β_z and β_θ are user defined. The default values are obtained by Marquette [18] from indirect comparisons to test (force coefficients) data reported by Kilgore (1988) [19], Iwatsubo (1990) [20], and Florjancic (1990) [13]. In Eqs, (6), V is the radial velocity of the flow at the interface between CVs II and III, U is the circumferential velocity, and W is the axial velocity [17, 18].

The sharp pressure drop (ΔP) at the inlet of the first land in a seal, known as a *Lomakin effect*, is

$$\Delta P = \frac{1 + \xi_{in}}{2} \rho W_o^2 \quad (8)$$

where W_o is the axial velocity at the entrance to the seal, the inlet loss coefficient ξ_{in} ranges from 0 to 0.2.

At the exit to the seal, the velocity head from the leakage flow may be converted into a pressure. This pressure recovery equals

$$\Delta P_{rise} = \frac{1 - \xi_{rec}}{2} \rho W_L^2 \quad (9)$$

where W_L is the exit axial velocity. Empirical values for the exit recovery factor ξ_{rec} range from 1 (no pressure recovery) to 0.7. Rotordynamic coefficients, particularly the direct stiffness coefficient, are sensitive to this parameter.

3.1 Predictions for Short Length Grooved Annular Seals

For short length seals ($L/D < 0.50$), XLCGrv® predictions give good correlation with test results [19]. In 1988, Kilgore [19] tested several *Halon* (CB_rF_3) lubricated plain (smooth surface) and circumferentially grooved seals operating with a high Reynolds number (pressure driven flow). Kilgore did not measure the inlet circumferential velocity U_o . In the data analysis, the rotordynamic coefficients \bar{K} , \bar{k} , \bar{C} , \bar{c} and \bar{M} are extracted from curve fits of the radial and tangential forces (f_r , f_θ) (per unit length) as a function of the whirl frequency Ω [17, 19]

$$f_r = -\bar{K} - \Omega \bar{c} + \Omega^2 \bar{M} \quad (10)$$

$$f_\theta = \bar{k} - \Omega \bar{C} \quad (11)$$

Table 1 shows the dimensions of two seals tested by Kilgore [19]. L_L and c , and L_g and c_g denote the land and groove length and depth, respectively. In seal 1, the grooves are shallow $c_g \sim c$. The appearance of a single vortex flow inside the cavity is questionable, however the predictions indicate that initial assumption of single-vortex flow inside the cavity remains valid as defined by three-control-volume model (shown in Figure 4 and Figure 5). For seal 7, the cavities are approximately square ($c_g/L_g = 1.0/1.6$).

Table 1 Dimensions of *Halon* seals tested by Kilgore [19]

$R = 50.42 \text{ mm}, L = 50.8 \text{ mm}$						
Seal #	Clearance, c (mm)	c_g (mm)	L_L (mm)	L_g (mm)	Number of Grooves	Average Groove Depth (*)
1	0.356	0.38	2.38	2.38	9	0.19
7	0.508	1.016	1.6	1.6	15	0.508

(*) Kilgore [19] uses an average groove depth not necessarily equal to the physical groove depth.

Figure 4 provides a comparison of the predicted and experimental results for the radial force f_r . There is good agreement between the predictions and experimental data for both seals over the whole range of pressure drop and shaft speed. Figure 5 presents similar results for the tangential force f_θ . Although the trend is correct, the model predictions tend to underestimate f_θ for seal 1, and overestimate it for seal 7 [17].

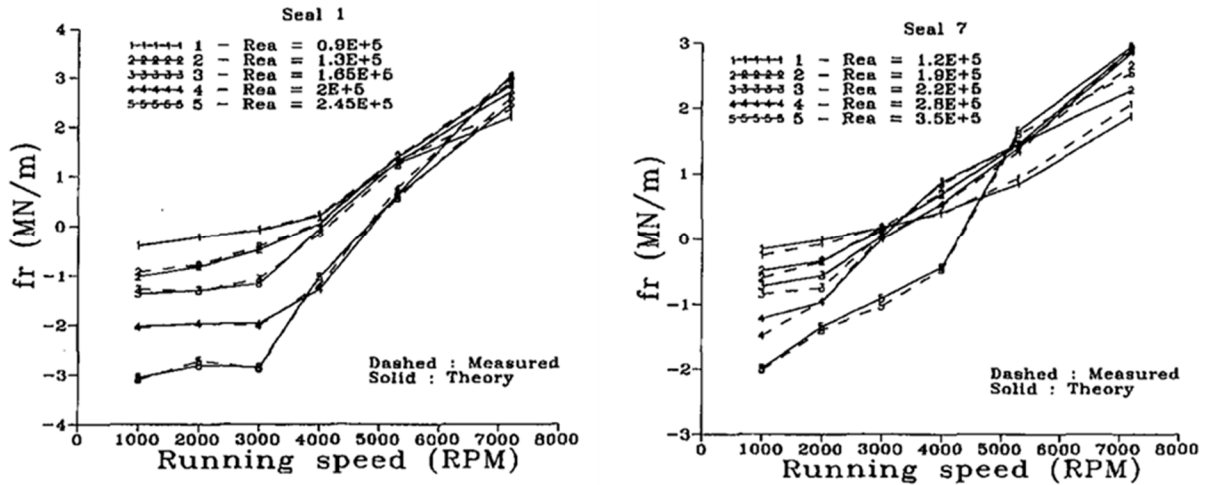


Figure 4. Experimental and predicted radial force (f_r) versus shaft speed for seals 1 and 7 in Kilgore [17].

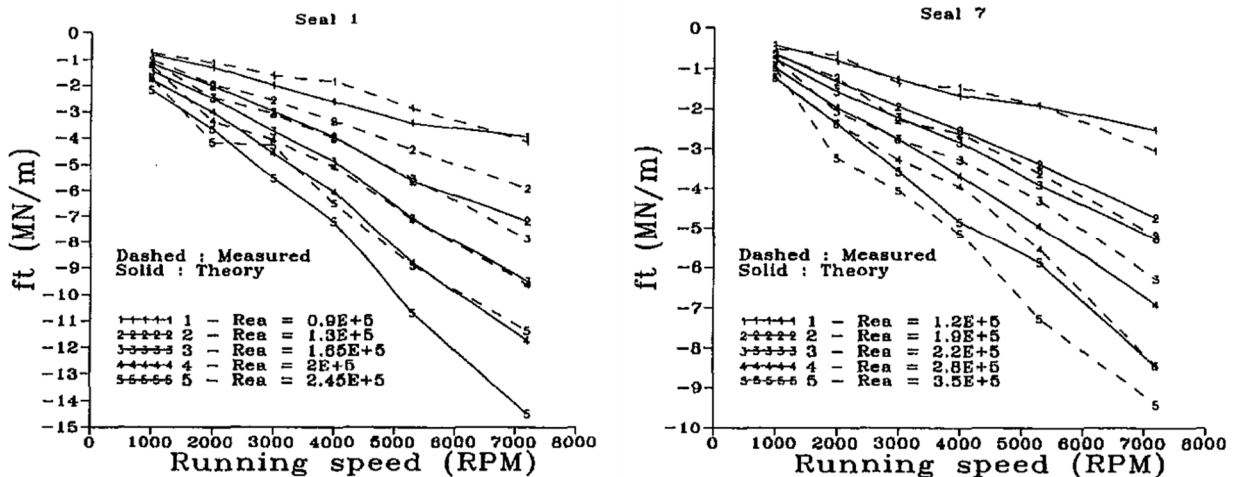


Figure 5. Experimental and predicted tangential force (f_θ) versus shaft speed for seals 1 and 7 in Kilgore [17].

With the experimentally determined parameters (n , m) for the friction coefficients derived from Kilgore' test results [19], the rotordynamic coefficients for the test short length grooved seals are reasonably well predicted. The direct stiffness is slightly under predicted. Direct damping is under predicted within 40%. Cross-coupled stiffness is accurately predicted [17].

3.2 Predictions for Long Grooved Annular Seals ($L/D > 1$)

The XLCGrv[®] program has friction factor coefficient's parameters (n , m) determined from tests conducted with short length seals [19], see prior section. There is no available test data from where to obtain adequate friction factor parameters for long seals. Presently, indirect comparison between predicted results of XLCGrv[®] and shop test results for a boiler feed pump indicates a poor correlation [6].

4. Analysis for Grooved Long Seal with CFD software

Nowadays commercial Computational Fluid Dynamics (CFD) software is widely available to simulate the flows in seals. In 2002, Villasmil *et al.* [1, 21] simulated the flat-plate-channel-flow experimental tests of water flowing with deliberately roughened surfaces by a 2D model with commercial CFD code. The predictions reveal an increase of friction factor with an increase in clearance. The higher friction factor characteristics of these deliberately roughened surfaces are governed by their ability to develop a high static pressure in the trailing face of each roughness cavity, while the wall shear stress on the smooth land plays a secondary role. In a certain Reynolds number range, the maximum friction factor observed on a specific roughness pattern size is independent of the actual clearance, referred to as the friction-factor-to-clearance indifference behavior. This phenomenon relates to the roughness cavity size and its length-to-clearance ratio. Villasmil *et al.* [22] devised the friction factor as [21, 23]:

$$f_f = \left[(4C_r)^3 \frac{\Delta P_x}{L_x} \rho(T) \right] * \frac{1}{\dot{m}_l^2} \quad (12)$$

$$Re = \frac{2}{[\mu(T)]} \dot{m}_l \quad (13)$$

where the expressions between brackets are extracted from the experimental data using a devised reverse procedure, and \dot{m}_l is the mass flow rate per unit width determined with the CFD software.

Villasmil's friction factors [1, 21] obtained with the 2D numerical approach are over predicted in comparison with the original experimental data. The difference between the predicted friction

factor and the experimental one could be up to 200%. Though the friction factors obtained from the 2D model are over predicted, the friction factor reproduces the well-known *jump effect* as the clearance varies, and above a threshold Reynolds number.

In 2003, Villasmil [23] extended the 2D approach to a 3D numerical analysis, which found that the texture's ability to develop high static pressures governs the friction factor of these surfaces. An exhaustive 3D numerical analysis of several experiments with liquid annular seals has been performed using a CFD code. Direct numerical simulations (DNS) of turbulent channel flow and smooth seals were replicated within 1% using Reynolds-averaged Navier-Stokes (RANS) equations and turbulence modeling. Similarly, measured groove seal leakage rates were reproduced within 2%. Villasmil's results reproduce the friction factor 'plateau' behavior predicted with the 2D analysis and observed in the flat plate experiments. Villasmil also reproduced the friction-factor-to-clearance indifference behavior; the maximum friction factor observed in a specific roughness pattern size is independent of the actual clearance in a certain Reynolds number range but clarifies the role of the roughness length-to-clearance ratio and the actual roughness size in defining the friction-factor-to-clearance proportionality. Villasmil's simulations indicate that textured surface area and roughness aspect ratios define the friction factor at a given seal clearance. The roughness pattern size, relevant to determine the friction-factor-to-clearance proportionality, plays a moderate role once the above cited ratios are defined. In any shape and size, shallow patterns are predicted and observed to provide larger friction factors than deep patterns. Villasmil's predictions also confirm limited experimental data, revealing that the mean flow orientation relative to the roughness pattern affects the friction factor.

In 2013, Untaroiu *et al.* [24] used 3D CFD method to predict the dynamic force coefficients for a long and grooved annular seal with a shallow groove depth $d_g/c=1.59/0.31$. Untaroiu *et al.* set the CFD model in a rotating frame of reference, the entire domain rotates with a whirling angular velocity Ω , the rotor spins with angular speed ω . Untaroiu *et al.* then calculate the fluid film forces acting on the rotor from the pressure distribution obtained by the CFD solution.

The linearized rotordynamic model describes the normal and tangential components of fluid forces acting on the rotor, as follows:

$$-\frac{F_x}{y} = -K_{xy} + C_{xx} \Omega + M_{xy} \Omega^2 \quad (14)$$

$$-\frac{F_y}{y} = K_{yy} + C_{yx} \Omega - M_{yy} \Omega^2 \quad (15)$$

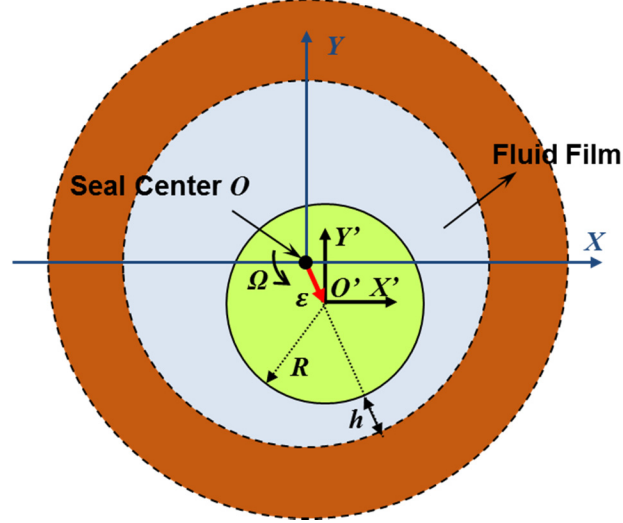


Figure 6. Cross section of seal with a whirling rotor

From Untaroiu's *et al.* [24], Table 2 lists the seal geometry, the boundary conditions and the flow parameters for the CFD simulation. Table 3 reproduces the predicted force coefficients derived from both the CFD solution and a bulk-flow method.

Table 2 Seal geometry, boundary conditions and flow parameters reproduced from Untaroiu *et al.* study [24]

L (mm)	D (mm)	S_{ax} (mm)	c (mm)	n -	L_g (mm)	L_l (mm)	c_g (mm)
267	224	9.95	0.31	20	3.18	9.53	1.59

Boundary conditions

	Inlet	Outlet	Rotor wall
V_z (m/s)	0.925		
V_θ (m/s)	35.49		
V_r (m/s)	0		
Pressure (Pa)		0	
Rotation speed (rpm)			3455
Whirl speed Ω (rpm)			[200,300,400,500,600]

	R (m)	V_θ (m/s)	ωR (m/s)	S	ΔP_{Model} (Pa)	ΔP_{Seal} (Pa)
Inlet model	0.183	35.49	66.39	0.54	1.8757×10^7	1.7964×10^7
Inlet seal	0.111	38.82	40.48	0.96	15	0.508

Table 3 Dynamic force coefficients from CFD and Bulk-Flow methods. Data reproduced from Untaroiu *et al.* study [24]

	CFD	Bulk flow method
$K_{xx} = K_{yy}$ (MN/m)	27.67	24.34
$K_{xy} = -K_{yx}$ (MN/m)	169.52	95.09
$C_{xx} = C_{yy}$ (KN s/m)	221.19	938.42
$C_{xy} = -C_{yx}$ (KN s/m)	245.88	250.4
$M_{xx} = M_{yy}$ (kg)	10.51	613.5
$M_{xy} = -M_{yx}$ (kg)	1436	-

The results reveal a reasonable correlation for the direct stiffness estimates, with the largest value predicted by CFD. In terms of cross-coupled stiffness, directly related to cross-coupled forces that contribute to rotor instability, the CFD also predicts the highest magnitude; however, a much larger discrepancy can be observed for this term (73% higher than the value predicted by the finite difference method and 79% higher than the bulk-flow code prediction). Similar large differences in predictions for damping and direct mass coefficients, where the bulk-flow methods predict the highest magnitudes [7, 24]. Note that the large magnitude $M_{xy} \sim 1,436$ kg (CFD solution) is clearly in error.

To validate the predictions from CFD method, Untaroiu *et al.* used the predicted dynamic force coefficients to estimate the rotor dynamic behavior of a pump. These estimations were then compared to the vibration characteristics measured during a shop test [24]. Table 4 lists the water pump operating conditions of the shop test.

Table 4 Pump operating conditions for Untaroiu et al. rotordynamic study [24]

Total differential head range (m)	970-1900
Rotational speed range (rpm)	2,550-3,570
Fluid specific gravity	1.0
Viscosity (cP)	1.0
Number of stages	9

The shop test results indicate that the coefficients predicted by CFD, when used in a rotordynamic analysis too, lead to close (and better) agreement with the manufacturer's pump test data. That is, the results of rotor dynamic analysis using the coefficients derived from CFD improved the prediction of both the damped natural frequency and damping factor for the fundamental first rotor-bearing mode, showing a substantially smaller damping factor than that derived from the shop test data, consistent with an experimentally observed instability of the rotor-bearing system [7].

Compared with the bulk flow model based method, the CFD approach could give accurate predictions for both short and long grooved seals by solving the complete Navier-Stokes equations with an appropriate turbulence flow model, thus avoiding the experimental determined friction factor coefficients and the assumptions applied in a three control volume bulk flow model.

5. A CFD/Bulk-Flow Hybrid Method

The bulk-flow theory, as developed by Hirs [8] for lubricant films, neglects the local velocity fluctuations due to flow turbulence and the shape of the velocity profile in favor of bulk mean fluid flow variables. Additionally, a bulk-flow analysis relates the wall shear stress to the bulk mean fluid velocity through a friction factor. These assumptions serve to simplify the governing equations and reduce the computational effort necessary in analyzing lubricant films [8].

However, bulk-flow theory requires a method of (empirical) evaluating accurately the friction factors from a myriad of operating conditions, and impractical enough, for a large number of (grove) configurations. With the friction factors determined by tests [14, 17, 19, 25], XLCGrv® can predict the rotordynamic coefficients for short length grooved seals with good accuracy and computational efficiency. Predictions of rotordynamic coefficients for a long annular seal with

shallow depth grooves are regarded as inadequate to reproduce field behavior in a boiler feed pump [7, 24].

When derived via CFD, predictions of rotordynamic coefficients for a long seal along with a rotordynamic analysis lead to a good correlation with shop and field pump tests. However, CFD approaches require of a significant computation time. For example, each of Untariou *et al.*'s 3D-CFD simulation for a grooved seal took ~ 13 hours [24].

6. Closure

This report discusses the fundamentals of the bulk-flow method and physics beyond the friction factor model approach, presents basic details on an existing bulk-flow code, XLCGrv®, for predictions rotordynamic force coefficients of annular seals with deep grooves. Recent predictions of force coefficients derived from CFD solutions are also presented.

XLCGrv® predictions of force coefficients have been benchmarked against test data for short length grooved seals. However, for long seals, an indirect comparison between the predictions of XLCGrv® and shop test indicates the predicted force coefficients are inadequate to reproduce field behavior in a boiler feed pump. Compared with the bulk-flow model, the CFD method has a high accuracy in predictions for the rotordynamic coefficients of long seals with either deep or narrow grooves. However, due to its complexity, typical CFD solutions demand of a large calculation time.

A CFD/bulk-flow hybrid method proves a good choice, considering both the computational efficiency and accuracy. Friction factors derived from a number of CFD simulations conducted for well-known balance piston (grooved seal) configurations will serve to update the bulk-flow software to deliver accurate force coefficients for ready implementation in reliable pump rotordynamic analyses.

In brief, the CFD software predicts the equilibrium flow field for sets of operating conditions and the walls' friction factors (f) are extracted. Difference friction factors, as numerical functions of changes in pressure ($\Delta f/\Delta P$), circumferential speed ($\Delta f/\Delta U$), and clearance ($\Delta f/\Delta c$), are inserted in the bulk-flow program to predict rotordynamic force coefficients. Untariou *et al.* [24] claim the method delivers great accuracy in predictions when comparing to test data (damping ratio) for a commercial pump, and with significant savings in computational time.

References

- [1] Villasmil Urdaneta, L., 2002, "Understanding The Friction Factor Behavior in Liquid Annular Seals with Deliberately Roughened Surfaces, A CFD Approach," M.S. Thesis, Mechanical Engineering, Texas A&M University, College Station.
- [2] Janson, W., Frei, A., and Florjancic, S., 1986, "Rotordynamic Coefficients and Leakage Flow of Parallel Grooved Seals and Smooth Seals," Accession Number: 87N22206, Rotordynamic Instability Problems in High-Performance Turbomachinery, NASA Lewis Research Center, pp. 129-153.
- [3] Childs, D. W., 1993, *Turbomachinery Rotordynamics: Phenomena, Modeling, and Analysis*, John Wiley & Sons, Chap. 4.
- [4] Adams, M. L., 2009, *Rotating Machinery Vibration: From Analysis to Troubleshooting*, CRC Press, Chap. 5.
- [5] Nordmann, R., Dietzen, F., and Weiser, H., 1989, "Calculation of Rotordynamic Coefficients and Leakage for Annular Gas Seals by Means of Finite Difference Techniques," ASME Journal of Tribology, **111**(3), pp. 545-552
- [6] TorishimaPumpR&D, 2014, "Validation of Rotor Stability Analysis by XLCGrv," Technical Report.
- [7] Untaroiu, A., Hayrapetian, V., Untaroiu, C. D., Wood, H. G., Schiavello, B., McGuire, J., 2013, "On the Dynamic Properties of Pump Liquid Seals," Journal of Fluids Engineering, **135**(5), pp.051104.
- [8] Hirs, G., 1973, "A Bulk-Flow Theory for Turbulence in Lubricant Films," Journal of Tribology, **95**(2), pp. 137-145.
- [9] San Andrés, L., 2010, Modern Lubrication Theory, "Turbulence Flow in Thin Film Bearings: Characteristics and Modeling," Notes 09, Texas A&M University Digital Libraries, <http://repository.tamu.edu/handle/1969.1/93197> [access date May 2015].
- [10] Massey, B. S., 1983, *Mechanics of Fluids*, Van Nostrand Reinhold (UK) Co. Ltd.
- [11] Nguyen, D., 1987, "Comparison of Hirs' Equation With Moody's Equation for Determining Rotordynamic Coefficients of Annular Pressure Seals 1," Journal of tribology, **109**, pp. 145.
- [12] Arghir, M., and Frene, J., 2004, " A Bulk-Flow Analysis of Static and Dynamic Characteristics of Eccentric Circumferentially Grooved Liquid Annular Seals," J. Tribolol., **126**(2), pp. 316-325.

- [13] Florjančič, Š., 1990, "Annular Seals of High Energy Centrifugal Pumps: A New Theory and Full Scale Measurement of Rotordynamic Coefficients and Hydraulic Friction Factors," Ph.D Thesis, Swiss Federal Institute of Technology, Zurich.
- [14] Kilgore, J., and Childs, D., 1990, "Rotordynamic Coefficients and Leakage Flow of Circumferentially Grooved Liquid Seals," *Journal of Fluids Engineering*, **112**(3), pp. 250-256.
- [15] Marquette, O., Childs, D., and San Andres, L., 1997, "Eccentricity Effects on The Rotordynamic Coefficients of Plain Annular Seals: Theory Versus Experiment," *Journal of Tribology*, **119**(3), pp. 443-447.
- [16] Scharrer, J. K., 1987, "A Comparison of Experimental and Theoretical Results for Labyrinth Gas Seals," M.S Thesis, Mechanical Engineering Department, Texas A & M University, College Station.
- [17] Marquette, O., and Childs, D., 1996, "An Extended Three-Control-Volume Theory for Circumferentially Grooved Liquid Seals," *ASME J. Tribol.*, **118**(2), pp. 276-285.
- [18] Marquette, O. R., 1994, "A New Three-Control-Volume Theory for Circumferentially-Grooved Liquid Seals," M.S Thesis, Mechanical Engineering, Texas A&M University, College Station.
- [19] Kilgore, J. J., 1988, "Rotordynamic Coefficients and Leakage Flow of Parallel-Grooved Liquid Seals," M.S Thesis, Mechanical Engineering, Texas A&M University, College Station.
- [20] Iwatsubo, T., and Sheng, B., 1990, "Evaluation of Dynamic Characteristics of Parallel Grooved Seals by Theory and Experiment," *Proc. Proceedings of the Third IFToMM International Conference on Rotordynamics*, Lyon, France, pp. 313-318.
- [21] Villasmil, L. A., Childs, D. W., and Chen, H.-C., 2005, "Understanding Friction Factor Behavior in Liquid Annular Seals with Deliberately Roughened Surfaces," *Journal of Tribology*, **127**(1), pp. 213-222.
- [22] Villasmil Urdaneta, L., Chen, H., Childs, D. W., 2003, "Evaluation of Near-wall Turbulence Models for Liquid Annular Seals with Roughened Walls," *AIAA 2003-3741*, 33rd AIAA Fluid Dynamics Conference and Exhibit, 23-26 June, 2003, Orlando, Florida

- [23] Villasmil, L. A., 2006, "Parameters Defining Flow Resistance and the Friction Factor Behavior in Liquid Annular Seals with Deliberately Roughened Surfaces," Ph.D Thesis, Mechanical Engineering, Texas A&M University, College Station.
- [24] Untaroiu, A., Untaroiu, C. D., Wood, H. G., Allaire, P. E., 2013, "Numerical Modeling of Fluid-Induced Rotordynamic Forces in Seals With Large Aspect Ratios," Journal of Engineering for Gas Turbines and Power, **135**(1), pp. 012501
- [25] Kanki, H., and Kawakami, T., 1988, "Experimental Study on The Static and Dynamic Characteristics of Screw Grooved Seals," Journal of Vibration and Acoustics, **110**(3), pp. 326-331.